Inorganic Chemistry

Article

Aβ$_{5−x}$ Peptides: N-Terminal Truncation Yields Tunable Cu(II) Complexes

Nina E. Wezynfeld, Aleksandra Tobolska, Mariusz Mital, Urszula E. Wawrzyniak, Magdalena Z. Wiloch, Dawid Płonka, Karolina Bossak-Ahmad, Wojciech Wróblewski, and Wojciech Bal*

Cite This: Inorg. Chem. 2020, 59, 14000−14011

Read Online

ACCESS | Metrics & More | Article Recommendations | Supporting Information

ABSTRACT: The Aβ$_{5−x}$ peptides (x = 38, 40, 42) are minor Aβ species in normal brains but elevated upon the application of inhibitors of Aβ processing enzymes. They are interesting from the point of view of coordination chemistry for the presence of an Arg-His metal binding sequence at their N-terminus capable of forming a 3-nitrogen (3N) three-coordinate chelate system. Similar sequences in other bioactive peptides were shown to bind Cu(II) ions in biological systems. Therefore, we investigated Cu(II) complex formation and reactivity of a series of truncated Aβ$_{5−x}$ peptide models comprising the metal binding site: Aβ$_{5−9}$, Aβ$_{5−12}$, Aβ$_{5−12}$Y10F, and Aβ$_{5−16}$. Using CD and UV−vis spectroscopies and potentiometry, we found that all peptides coordinated the Cu(II) ion with substantial affinities higher than 3×10^{12} M$^{−1}$ at pH 7.4 for Aβ$_{5−9}$ and Aβ$_{5−12}$. This affinity was elevated 3-fold in Aβ$_{5−16}$ by the formation of the internal macrochelate with the fourth coordination site occupied by the imidazole nitrogen of the His13 or His14 residue. A much higher boost of affinity could be achieved in Aβ$_{5−9}$ and Aβ$_{5−12}$ by adding appropriate amounts of the external imidazole ligand. The 3N Cu-Aβ$_{5−x}$ complexes could be irreversibly reduced to Cu(I) at about −0.6 V vs Ag/AgCl and oxidized to Cu(III) at about 1.2 V vs Ag/AgCl. The internal or external imidazole coordination to the 3N core resulted in a slight destabilization of the Cu(I) state and stabilization of the Cu(III) state. Taken together these results indicate that Aβ$_{5−x}$ peptides, which bind Cu(II) ions much more strongly than Aβ$_{1−x}$ peptides and only slightly weaker than Aβ$_{4−x}$ peptides could interfere with Cu(II) handling by these peptides, adding to copper dyshomeostasis in Alzheimer brains.
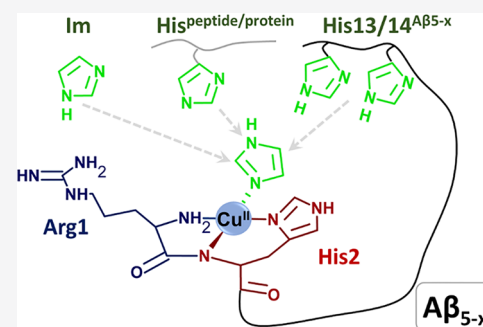
INTRODUCTION

Alzheimer's disease (AD) accounts for approximately 50−70% cases of dementia, over 50 million people worldwide.[1,2] Amyloid-β (Aβ) peptides are at the center of AD pathology. They compose amyloid plaques, a historic hallmark of the disease, and were more recently demonstrated to form neurotoxic oligomers.[3,4] Aβ peptides are derived from the amyloid precursor protein (APP), which undergoes alternative proteolytic cleavage pathways in amyloidogenic and non-amyloidogenic processes. In the amyloidogenic pathway APP is cleaved by β-secretase (BACE1), a membrane-anchored aspartyl protease which cleaves APP before position 1 of the Aβ domain, and γ-secretase, a membrane-bound protease complex responsible for creation of the Aβ C-terminus.[5] The Aβ$_{1−40}$ and Aβ$_{1−42}$ peptides formed in this pathway are further processed hydrolytically to N-terminally truncated species, which represent more than 60% of all Aβ species in AD brains. Aβ$_{4−42}$ is the most abundant of these peptides.[6−9] Another is Aβ$_{5−42}$, detected in Aβ deposits in brains of sporadic and familial AD victims and in transgenic mouse models.[9−11]

The origin of Aβ$_{5−x}$ species (x = 38, 40, 42) is unclear. They were shown to be elevated in the course of application of inhibitors of BACE1 in experimental animals.[5,12] This suggests direct alternative cleavage of APP, becoming possible when the main pathway is inhibited. They can also be produced by caspases, largely cellular apoptotic proteases implicated in AD neurodegeneration.[13]

Aβ$_{5−x}$ peptides contain His in the second position (Xaa-His). Such Xaa-His arrangement creates a specific Cu(II) binding site distinct from both the dynamic ensemble of macrochelate species of Aβ$_{1−x}$ peptides[14,15] and the rigid ATCUN/NTS chelate system of Aβ$_{4−x}$ peptides.[16−18] The basic structure of Xaa-His-Zaa cupric complexes, derived from X-ray studies of Gly-His-Lys (GHK) and spectroscopic studies of many oligopeptides bearing various Xaa substitutions is three-coordinate, with the Xaa N-terminus, the Xaa-His peptide bond, and the His imidazole providing three nitrogen ligands arranged in a square-planar fashion around the Cu(II) ion (3N species). The fourth position can be occupied by a
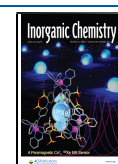
water molecule or other ligands, such as imidazoles or carboxylates from other peptide molecules, phosphate ions, etc.[19−21] The amino acid residue directly following His (Zaa in Xaa-His-Zaa... sequences) cannot participate in the coordination for sterical reasons. The stability constants available in the literature indicate that the effective stability constants of Cu(II) complexes of Xaa-His-Zaa peptides are in the range of $10^{12}–10^{13}$ M^{-1}, slightly less than those of ATCUN/NTS motifs.[18,21−23] We demonstrated, however, that at a sufficiently high concentration of the ternary ligand the effective stability constants of such a ternary XHZ-Cu(II)-L complex may be elevated by one or 2 orders of magnitude.[20]

In this work, we aimed to characterize Cu(II) coordination and electrochemical properties of resulting complexes, $A\beta_{5-x}$ peptides, by using $A\beta_{5-16}$ as a suitable well-soluble model, analogously to $A\beta_{1-16}$ and $A\beta_{4-16}$ model peptides.[15,16] Because of the presence of two metal binding regions in this peptide, one at the N-terminus and another at the His13-His14 couple, we also used shorter peptides, $A\beta_{5-9}$ and $A\beta_{5-12}$ as simplified models. For a better understanding of the role of Tyr10 in the studied processes, we also used a modified $A\beta_{5-12}Y10F$ ($A\beta_{5-12F}$) peptide in some experiments (see Scheme 1 for

Scheme 1. Sequences of $A\beta_{5-x}$ Peptides Studied in This Work[a]

$A\beta_{5-9}$	RHDSG−NH$_2$
$A\beta_{5-12}$	RHDSGYEV−NH$_2$
$A\beta_{5-12F}$	RHDSGFEV-NH$_2$
$A\beta_{5-16}$	RHDSGYEVHHQK−NH$_2$

[a]Residues whose side chains contribute to Cu(II) binding are highlighted in red (His) and blue (Tyr).

sequences). Spectroscopic (UV−vis, CD, fluorescence) and potentiometric experiments were used to decipher and quantify the set of complex species formed in a broad pH range, while their redox properties were investigated using voltammetry (CV and DPV). Then, spectroscopic and electrochemical titrations of Cu(II)-$A\beta_{5-x}$ complexes with imidazole, a model of His residues in proteins, were employed to estimate the influence of such interactions on the stability and reactivity of studied complexes. The obtained quantitative description allowed us to assess the potential role of $A\beta_{5-x}$ peptides in copper physiology in the brain.

■ EXPERIMENTAL METHODS

Materials. N-α-9-Fluorenylmethyloxycarbonyl (Fmoc) amino acids were purchased from Novabiochem. Trifluoroacetic acid (TFA), piperidine, and N,N,N′,N′-tetramethyl-O-(1H-benzotriazol-1-yl)uronium hexafluorophosphate (HBTU) were obtained from Merck. Triisopropylsilane (TIS), N,N-diisopropylethylamine (DIEA), 4-(2-hydroxyethyl)piperazine-1-ethanesulfonic acid (HEPES), CuCl$_2$, Cu(NO$_3$)$_2$·H$_2$O, NaOH, KOH, HCl, KNO$_3$, HNO$_3$, and imidazole were from Sigma. The TentaGel S RAM resin was purchased from RAPP Polymere. Diethyl ether and dichloromethane (DCM) were from Chempur. Acetonitrile and calibrated 0.1 M NaOH solution for potentiometry were from POCH, and dimethylformamide (DMF) was from Roth.

Peptide Synthesis. $A\beta_{5-16}$(RHDSGYEVHHQK-NH$_2$), $A\beta_{5-12}$(RHDSGYEV-NH$_2$), $A\beta_{5-9}$(RHDSG-NH$_2$), and $A\beta_{5-12F}$ (RHDSGFEV-NH$_2$) were synthesized by solid-phase peptide synthesis using a CEM Liberty microwave peptide synthesizer (Applied Biosystems) according to a Fmoc/tBu protocol with HBTU and

DIEA as coupling reagents and 20% piperidine in DMF as a Fmoc removal agent.[24] TentaGel S RAM resin was used as a solid phase. The peptides were cleaved from the resin in TFA/TIS/water 95:2.5:2.5 v/v/v for 2 h. Then, the peptides were precipitated with cold diethyl ether, centrifugated, dissolved in water, and lyophilized. The crude peptides were purified by HPLC (Waters) following a detection at 220 nm/280 nm using a mix of eluting solvents A (0.1% (v/v) TFA in water) and B (0.1% (v/v) TFA in 90% (v/v) acetonitrile). The purification method was a gradient of eluents 5−45% of B within 40 min, flow 2 mL/min. The mass of the pure peptides was further verified by ESI-MS. The concentrations of initial peptide stock solutions were determined by potentiometric titrations. Concentrations of secondary and subsequent stock solutions of $A\beta_{5-12}$ and $A\beta_{5-16}$ were determined using an extinction coefficient ε of 1375 M^{-1} cm^{-1} at 275 nm. For $A\beta_{5-12F}$ and $A\beta_{5-9}$ ε values of 200 M^{-1} cm^{-1} at 258 nm and ε of 9032 M^{-1} cm^{-1} at 214 nm were used.[25]

UV−vis, CD, and Fluorescence Spectroscopy. The UV−vis spectra were obtained on a PerkinElmer spectrophotometer over the spectral range of 200−900 nm. The circular dichroism (CD) spectra were recorded over the range of 250−800 nm on a Jasco 815 spectropolarimeter. All spectroscopic measurements were performed at 25 °C in a 1 cm path length quartz cuvette.

Titrations with NaOH (pH dependence): Samples containing 1 mM $A\beta$ ($A\beta_{5-9}$, $A\beta_{5-12}$, $A\beta_{5-12F}$, $A\beta_{5-16}$), and 0.9 mM Cu(II) or 1 mM $A\beta$ ($A\beta_{5-16}$) and 1.8 mM Cu(II) were titrated with a small portion of concentrated NaOH in the pH range 2.5−10.

Titrations with imidazole/$A\beta_{5-9}$/$A\beta_{1-16}$: Samples containing 1 mM $A\beta$ ($A\beta_{5-9}$, $A\beta_{5-12}$, $A\beta_{5-12F}$, $A\beta_{5-16}$) and 0.8 mM Cu(II) at pH 7.4 were titrated with a small portion of imidazole/$A\beta_{5-9}$/$A\beta_{1-16}$ stock solution. The pH of the sample was strictly controlled during the experiment and adjusted if necessary.

Kinetic Experiment. $A\beta_{4-9}$ was added to the sample containing 0.9 mM Cu(II) and 1 mM $A\beta_{5-9}$ in 20 mM HEPES pH 7.4 to the final $A\beta_{4-9}$ concentration of 1 mM. The changes in UV−vis spectra were monitored for 24 h.

Fluorescence spectra were registered using a Cary Eclipse spectrofluorimeter (Varian) with the excitation wavelength of 275 nm and detection of emission in the range of 280−400 nm. All fluorescence measurements were performed at 25 °C in a 1 cm path length quartz cuvette. The samples of 20 μM $A\beta_{5-12}$ or 20 μM $A\beta_{5-12}$/19 μM CuCl$_2$ were titrated with NaOH from pH 4.2 to 12.2.

The pK values were calculated using Hill equations eq 1 and eq 2:
(i) for a single process

$$F = \frac{p_1 + p_2 \times 10^{n(pH-pK)}}{1 + 10^{n(pH-pK)}} \tag{1}$$

(ii) for a two-step process

$$F = \frac{p_1 + p_x \times 10^{n_1(pH-pK_1)} + p_2 \times 10^{n_1(pH-pK_1)+n_2(pH-pK_2)}}{1 + 10^{n_1(pH-pK_1)+n_2(pH-pK_2)}} \tag{2}$$

where F stands for spectroscopic intensity at given pH; p_1 and p_2 stand for spectroscopic intensity for the fully protonated or deprotonated state, respectively; p_x stands for the spectroscopic intensity of the first step in the two-step process; and n, n_1, and n_2 stand for Hill coefficients.

Potentiometry. Potentiometric titrations were performed on a Titrando 907 automatic titrator (Metrohm) using a combined glass-Ag/AgCl electrode (InLabMicro, Mettler Toledo, Switzerland). The electrode was calibrated daily by titrating nitric acid.[26] The CO$_2$-free solution of 0.1 M NaOH was used as the titrant. All experiments were performed under argon at 25 °C. Sample volumes were 1.5 mL. The samples contained 1.0 mM $A\beta$ peptide ($A\beta_{5-16}$, $A\beta_{5-12}$, $A\beta_{5-9}$) dissolved in 4 mM HNO$_3$/96 mM KNO$_3$. The Cu(II) complex formation was studied for the different peptide:metal stoichiometries (1:2, 1:1, 1:0.5) using a 5−10% excess of peptides over metal ions, over the pH range from 2.3 to 12.2. SUPERQUAD and HYPERQUAD were used to analyze the data.[27,28] At least three titrations

were performed separately to determined the protonation and Cu(II) stability constants of the studied compounds.

Voltammetry. The electrochemical experiments were done in a three-electrode arrangement with Ag/AgCl as the reference, platinum wire as the counter, and glassy carbon electrode (GCE, BASi, 3 mm diameter) as the working electrode. The reference electrode was separated from the working solution by an electrolytic bridge filled with 4 mM HNO_3/96 mM KNO_3 solution. The GC electrode was sequentially mechanically polished with 1.0 and 0.3 μm alumina powder on a Buehler polishing cloth to a mirror-like surface. In order to remove the remaining powder, the electrode was sonicated for 1 min in deionized water. All electrochemical measurements were carried out in 96 mM KNO_3 solutions containing 4 mM HNO_3 solution at pH 7.4. The pH was adjusted by adding small volumes of concentrated KOH or HNO_3 solutions; the concentrations of peptides were 0.5 mM and the ligand-to-Cu(II) ratio was 1:0.8 in all cases (a small Cu(II) deficiency was applied to avoid the interference from uncomplexed Cu(II) cations). In ternary complex investigations imidazole was added to the Cu(II)−peptide complex up to 10 mM concentration. The pH was closely controlled before, during, and at the end of each voltammetric measurement. Oxygen was removed from the sample solution by passing argon for 5−10 min before all measurements, and an argon blanket was maintained over the solution during the experiments carried out at 25 °C.

Cyclic (CV) and differential pulse voltammetry (DPV) experiments were performed using the CHI 1030 potentiostat (CH Instrument, Austin, USA). For all presented CV curves, the scan rate (ν) was 100 mV/s. The following parameters were used in DPV: pulse amplitude 50 mV, pulse time 100 ms.

■ RESULTS AND DISCUSSION

Aβ_{5-9} Complexes. We first performed a set of pH-metric titrations of the studied peptides in the absence and presence of Cu(II) ions. The protonation constants calculated from these experiments are presented in Table 1. The assignments of proton exchanging groups mainly contributing to given

Table 1. Protonation Constants (log β^a and pK_a Values) of Aβ_{5-9}, Aβ_{5-12}, and Aβ_{5-16} (L) at I = 0.1 M (KNO_3), Determined by Potentiometry at 25 °C[b,16,29,30]

Species	Log β^a	pK_a	Assignment
Aβ_{5-9}			
HL	7.37(1)	7.37	Arg5 N-term.
H_2L	13.51(1)	6.13	His6
H_3L	16.67(1)	3.17	Asp7
Aβ_{5-12}			
HL	10.08(1)	10.08	Tyr10
H_2L	17.60(1)	7.52	Arg5 N-term.
H_3L	23.84(1)	6.25	His6
H_4L	28.21(1)	4.37	Glu11
H_5L	30.94(1)	2.73	Asp7
Aβ_{5-16}			
HL	10.39(1)	10.39	Tyr10/Lys16
H_2L	20.35(1)	9.96	
H_3L	27.94(1)	7.60	Arg5 N-term.
H_4L	34.61(1)	6.67	His6/13/14
H_5L	40.92(1)	6.31	
H_6L	46.43(1)	5.50	
H_7L	50.35(1)	3.92	Glu11
H_8L	52.83(1)	2.48	Asp7

[a]$\beta(H_nL) = [H_nL]/([L][H^+])_n$. [b]Standard deviations on the last digits provided by HYPERQUAD,[28] given in parentheses, represent statistical errors of constant determinations. Assignments are based on literature values.

protonation constants are based on previous studies of analogous peptides.[16,29,30] The pK_a values are typical for the respective groups and sufficiently well separated to make these assignments unambiguous.[31]

The potentiometric titrations performed at various Cu(II)/peptide ratios for Aβ_{5-9} indicated the formation of complexes having solely a 1:1 copper-to-peptide stoichiometry and differing by the number of bound/released hydrogen ions (Table 2). The CD and UV−vis spectra of Cu(II)-Aβ_{5-9}

Table 2. Stability Constants (log β^a and pK_a Values) of Cu(II) Complexes of Aβ_{5-9}, Aβ_{5-12}, and Aβ_{5-16} (L) at I = 0.1 M (KNO_3), Determined by Potentiometry at 25 °C[b]

Species	Log β^a	pK_a	Assignment	Coordination Mode
Aβ_{5-9}				
CuL	9.48(1)			$3N+H_2O$
$CuH_{-1}L$	5.66(1)	3.82	Asp7	$3N+H_2O$
$CuH_{-2}L$	−3.69(1)	9.35	Equatorial H_2O	$3N+OH^-$
Total 3N +H$_2$O		3.61		$3N+H_2O$
Aβ_{5-12}				
CuH_2L	23.72(3)			$3N+H_2O$
CuHL	20.44(1)	3.23	Asp7	$3N+H_2O$
CuL	15.76(1)	4.69	Glu11	$3N+H_2O$
$CuH_{-1}L$	6.29(2)	9.47	Tyr10/H_2O	3N/Tyr10 and $3N+OH^-$
$CuH_{-2}L$	−3.76(2)	10.05	H_2O/Tyr10	$3N+OH^-$
Total 3N +H$_2$O		3.66		
Aβ_{5-16}				
CuH_5L	46.00(2)			$3N+H_2O$
CuH_4L	42.79(1)	3.212	Asp7	$3N+H_2O$
CuH_3L	38.62(1)	4.169	Glu11	$3N+H_2O$
CuH_2L	33.46(1)	5.159	His13/14	$3N+N$
CuHL	26.11(2)	7.35	His13/14	$3N+N$
CuL	16.43(3)	9.68	Equatorial H_2O/Tyr10/Lys16	$3N+N/3N+OH^-$
$CuH_{-1}L$	6.56(3)	9.87		
$CuH_{-2}L$	−3.38(2)	9.94		
Cu_2HL	31.50(1)			
Cu_2L	25.37(1)	6.134	His13/14 N^-	$3N+H_2O + 2N$
$Cu_2H_{-1}L$	19.08(1)	6.29		$3N+H_2O + 3N$
$Cu_2H_{-2}L$	10.15(1)	8.93	Val12/Glu11 N^-	$3N+H_2O + 4N$
$Cu_2H_{-3}L$	1.05(1)	9.1	Equatorial H_2O	3N/OH- + 4N
$Cu_2H_{-4}L$	−9.4(1)	10.45	Lys16/Tyr10	3N/OH- + 4N
$Cu_2H_{-5}L$	−19.94(9)	10.54		3N/OH- + 4N
Total 3N +H$_2$O		3.62		

[a]$\beta(Cu_mH_nL) = [M_mH_nL]/([M]_m[L][H^+]_n)$. [b]Standard deviations on the last digits provided by HYPERQUAD,[28] given in parentheses, represent statistical errors of constant determinations. Assignments are based on literature values.[20,21,29,30] Coordination modes are derived from the analysis presented below.

complexes are presented in Figures 1 and S1, respectively. Figure 2 demonstrates the potentiometric species distribution compared to parameters derived from these spectra. The quantitative agreement of these results allowed us to calculate the spectroscopic parameters for individual complexes, as given in Table 3. The first complex formed is a 3N species with spectroscopic parameters analogous to those recorded earlier for GHK, WHWSKNR-NH$_2$, and GHTD-NH$_2$ peptides,[19−23] with the fourth equatorial site occupied by a water molecule. It
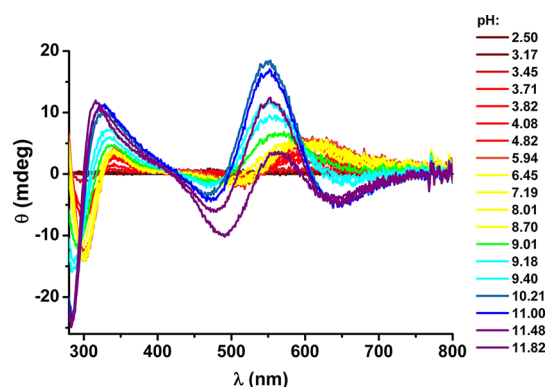
Figure 1. pH dependence of CD spectra recorded at 25 °C for 0.9 mM Cu(II) and 1.0 mM $A\beta_{5-9}$, at pH values color coded on the graphs.
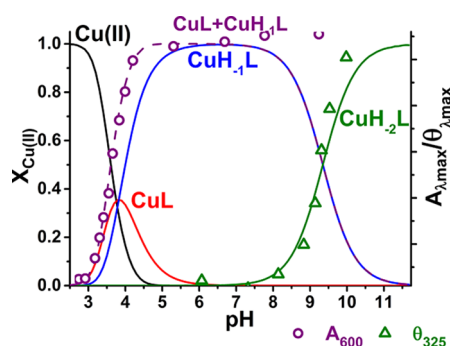

Figure 2. Species distribution calculated for 0.9 mM Cu(II) and 1.0 mM $A\beta_{5-9}$, on the basis of constants presented in Tables 1 and 2, with selected spectroscopic parameters overlaid.

contains two spectroscopic forms, CuL and $CuH_{-1}L$, differing by deprotonation of the Asp7 side chain carboxyl function. This event, recorded by potentiometry with the pK_a of 3.82, does not affect the spectroscopic parameters (Tables 2 and 3). It is not surprising, as the coordination of the Asp7 carboxylate to the Cu(II) ion bound in the 3N core provided by Arg5 and His6 is excluded by the complete geometry. The elevation of Asp7 pK_a by 0.65 pH units can be explained by lowering the overall molecular charge by Cu(II) coordination by one, compared to the unbound peptide.

The next recorded deprotonation occurred with the pK_a of 9.35 and was associated by a significant blue shift of the $d−d$ band maximum, the change of its symmetry in CD, and concomitant alterations in charge transfer bands (Figure 1, Table 3). These changes are due to the deprotonation of the coordinated water molecule.[20,21] The additional split in the $d−d$ band, not observed in titrations of WHWSKNR-NH₂ and GHTD-NH₂ complexes,[19,20] is indicative of an additional interaction involving the coordinated hydroxyl anion, most likely with the cationic Arg side chain.

At still higher pH above 10 a further set of changes appeared in the CD spectra, with a characteristic strong negative feature at 500 nm. According to the literature, they are due to the replacement of the hydroxyl group by the deprotonated $N\tau$ of the imidazole ring, possibly resulting in imidazole-bridged oligomers.[21,32,33]

The potentiometric titrations did not provide evidence for the presence of a CuL_2-type complex. Such complexes were reported previously for simpler XHZ peptides by potentiometry, but with little support by independent direct techniques

Table 3. Spectroscopic Parameters for Cu(II) Mono-complexes of $A\beta_{5-x}$ Peptides at 25 °C

Complex	Mode (species)	UV−vis λ_{max}/nm (ε/M^{-1} cm^{-1})	CD λ_{ext}/nm ($\Delta\varepsilon$/M^{-1} cm^{-1})
Cu(II)-$A\beta_{5-9}$	3N+H₂O (CuL + CuH$_{-1}$L)	600 (47)[a]	600 (+0.17)[a]
			505 (−0.05)[a]
			341 (+0.12)[b]
			300 (−0.46)[c]
			267 (+0.53)[d]
	3N+OH⁻ (CuH$_{-2}$L)	555 (63)[a]	650 (−0.1)[a]
			546 (+0.61)[a]
			470 (−0.11)[a]
			325 (+0.38)[b,c]
			285 (−0.76)[d]
Cu(II)-$A\beta_{5-12}$	3N+H₂O (CuH₂L +CuHL+CuL)	600 (60)[a]	600 (+0.14)[a]
			503 (−0.05)[a]
			341 (+0.09)[b]
			301 (−0.37)[c]
	3N/Tyr10 and 3N+OH⁻ (CuH$_{-1}$L)	560 (89)[a]	650 (−0.09)[a]
		400sh (82)[e]	548 (+0.29)[a]
			470 (−0.09)[a]
			400 (+0.09)[e]
			325 (+0.25)[b]
Cu(II)-$A\beta_{5-12F}$	3N+H₂O	600 (60)[a]	605 (+0.16)[a]
			513 (−0.05)[a]
			341 (+0.08)[b]
			301 (−0.39)[c]
	3N+OH⁻	555 (85)[a]	650 (−0.08)[a]
			553 (+0.44)[a]
			470 (−0.09)[a]
			323 (+0.28)[b,c]
			283 (−0.64)[d]
Cu(II)-$A\beta_{5-16}$	3N+H₂O (CuH₅L +CuH₄L+CuH₃L)	600 (58)[a]	605 (+0.19)[a]
			506 (−0.05)[a]
			341 (+0.11)[b]
			301 (−0.47)[c]
	3N+N (CuH₂L+ CuHL)	565 (66)[a]	640 (−0.05)[a]
			553 (+0.16)[a]
			478 (−0.09)[a]
			336 (+0.12)[b]
			300 (−0.35)[c]
	3N+OH⁻ (CuL+CuH$_{-1}$L +CuH$_{-2}$L)	560 (73)[a]	640 (−0.07)[a]
			553 (+0.20)[a]
			478 (−0.10)[a]
			336 (+0.17)[b,c]

[a] $d−d$ transition. [b] $N^{im}−Cu^{II}$ charge transfer (CT). [c] $N^{-}−Cu^{II}$ CT. [d] $N^{am}−Cu^{II}$ CT. [e] Tyr $O^{-}−Cu^{II}$ CT.

in solution.[17,19,23,32−35] No such complex was detected for WHWSKNR-NH₂. It was also invisible for potentiometry in the study of GHTD-NH₂ complexes, due to insufficient stability at submillimolar peptide concentrations, but a spectroscopic titration with the peptide excess demonstrated its existence at pH 7.4.[21] Here we used the same approach to detect it, as shown in Figure 3. The associated spectral changes were very similar to those observed for GHTD-NH₂, indicating the formation of a 3 + 1N complex, with the water molecule replaced by an imidazole nitrogen of the second peptide molecule. The conditional stability constant derived from this titration is provided in Table 4, and the spectral parameters of
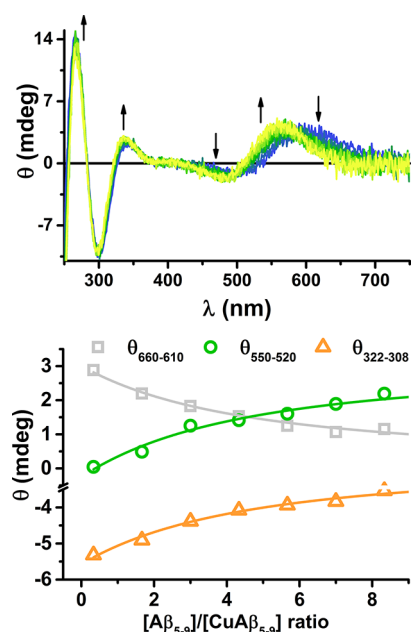
Figure 3. Top: the titration of 0.8 mM Cu(II) and 1.0 mM $A\beta_{5-9}$ at 25 °C and pH 7.4 with the excess of $A\beta_{5-9}$, up to 15 mM, monitored by CD. Arrows mark the direction of changes. Bottom: the fit of the conditional stability constant of the CuL_2 complex at spectral areas of maximum change: 635 nm (gray), 535 nm (green), and 315 nm (orange).

this complex are given in Table 5, along with the parameters of ternary complexes with imidazole.

Table 4. Conditional Stability Constants (M^{-1}) for Binary ($^{C}K_{7.4}$) and Ternary ($^{T}K_{7.4}$) for Cu(II) Complexes of $A\beta_{5-x}$ Peptides at pH 7.4[a]

| Peptide | $^{C}K_{7.4}$ | $^{T}K_{7.4}$ | | |
		imidazole	$A\beta_{5-9}$	$A\beta_{1-16}$
$A\beta_{5-9}$	5.75×10^{12}	870 ± 69	283 ± 50	5200 ± 200
$A\beta_{5-12}$	5.13×10^{12}	557 ± 36	n.a.	n.a.
$A\beta_{5-16}$	9.55×10^{12}	98 ± 27	n.a.	n.a.

[a]$^{C}K_{7.4}$ values were calculated from potentiometric data using the CI approach. Competitivity index (CI) was calculated for Cu(II), peptide, and ligand (Z) concentrations of 0.001 M. CI is the value of log K_{CuZ} such as the condition $\sum_{ijk}([Cu_iH_jL_k]) = [CuZ]$ is fulfilled, where Z is a theoretical competitor.[39] n. a. stands for not analyzed. $^{T}K_{7.4}$ were calculated directly from spectroscopic titrations using eq 1.

$A\beta_{5-12}$ and $A\beta_{5-12F}$ Complexes. The extension of the sequence by residues 10–12, YEV, added two proton-exchanging side chains, Tyr10 and Glu11 in $A\beta_{5-12}$. Their characteristic pK_a values about 10 and 4, respectively, together with the data for $A\beta_{5-9}$, allowed us to directly assign the respective protonation events to individual groups, as provided in Table 1 and presented in Figure 4.

Accordingly, the lowest-pH complex of $A\beta_{5-12}$ has the CuH_2L stoichiometry, but the same 3N coordination as the CuL complex of $A\beta_{5-9}$, as seen in CD and UV–vis spectra, presented in Figures 5A and S2, respectively. The next two deprotonations under pH 5 did not affect the spectra and can be assigned to Asp7 and Glu11 carboxyl deprotonations. The spectra became more complicated above pH 8, where two overlapping deprotonations took place. In order to facilitate

Table 5. Spectroscopic Parameters of Ternary Complexes of Cu(II)-$A\beta_{5-x}$ with Imidazole (Im) or $A\beta_{5-x}$ at 25 °C

| Ternary complex | Mode | UV–vis | CD |
		λ_{max}/nm (ε/M^{-1} cm^{-1})	λ_{ext}/nm ($\Delta\varepsilon$/M^{-1} cm^{-1})
Cu(II)-$A\beta_{5-9}$+ $A\beta_{5-9}$	$3N+N_{A\beta(5-9)}$	566 (79)[a]	560 (+0.20)[a]
			478 (−0.08)[a]
			335 (+0.15)[b]
			300 (−0.37)[c]
			267 (+0.51)[d]
Cu(II)-$A\beta_{5-9}$+ $A\beta_{1-16}$	$3N+N_{A\beta(1-16)}$	575 (76)[a]	564 (+0.22)[a]
			482 (−0.07)[a]
			337 (+0.17)[b]
			298 (−0.37)[c]
Cu(II)-$A\beta_{5-9}$+ Im	$3N+N^{Im}$	566 (75)[a]	645 (−0.11)[a]
			551 (+0.17)[a]
			478 (−0.08)[a]
			332 (+0.11)[b]
			296 (−0.35)[c]
			265 (+0.54)[d]
Cu(II)-$A\beta_{5-12}$+ Im	$3N+N^{Im}$	562 (81)[a]	644 (−0.11)[a]
			550 (+0.17)[a]
			478 (−0.11)[a]
			333 (+0.13)[b]
			297 (−0.40)[c]
Cu(II)-$A\beta_{5-16}$+ Im	$3N+N^{Im}$	564 (70)[a]	645 (−0.08)[a]
			553 (+0.19)[a]
			478 (−0.06)[a]
			330 (+0.12)[b]
			297 (−0.35)[c]

[a]d–d transition. [b]N^{im}–Cu^{II} charge transfer (CT). [c]N^{-}–Cu^{II} CT. [d]N^{am}–Cu^{II} CT.
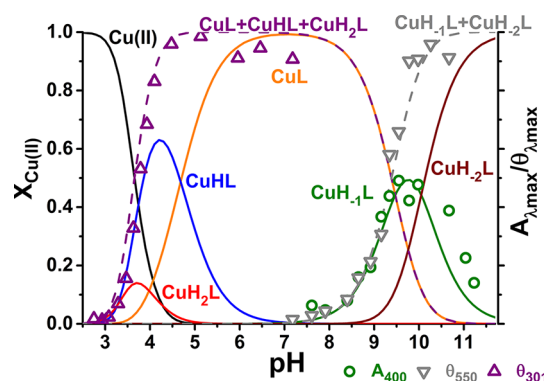

Figure 4. Species distribution calculated for 0.9 mM Cu(II) and 1.0 mM $A\beta_{5-12}$, on the basis of constants presented in Tables 1 and 2, with selected spectroscopic parameters of $A\beta_{5-12}$ overlaid.

the analysis, we performed spectroscopic titrations of Cu(II)-$A\beta_{5-12F}$, the analog having Tyr replaced with Phe. The respective CD and UV–vis results are presented in Figures 5B and S3.

The pK_a values for the 3N complex formation obtained from CD titrations were 3.77(1) and 3.51(2) for the formation of 3N complexes of $A\beta_{5-12}$ and $A\beta_{5-12F}$, respectively. The former value is in a good agreement with the potentiometry-derived value of 3.66. Based on the characteristic CT band at 400 nm, seen particularly clearly in UV–vis spectra of Cu(II)-$A\beta_{5-12}$ contrasted with Cu(II)-$A\beta_{5-12F}$ in the pH range 7–10 (Figure 6A) and CD titrations monitored at 370–380 nm (Figure 6B),
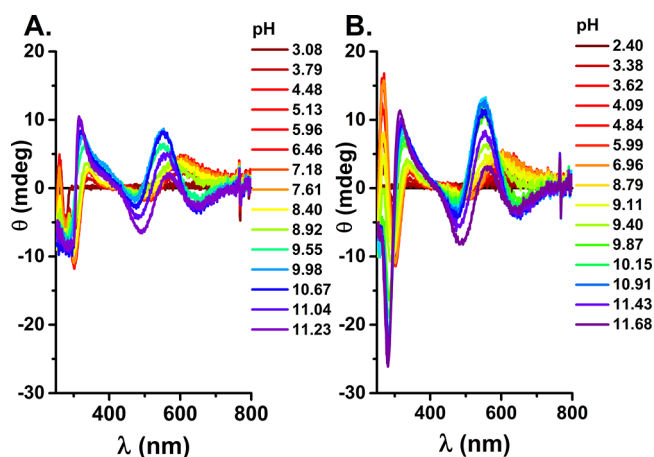
Figure 5. CD spectra recorded at 25 °C for 0.9 mM Cu(II) and 1.0 mM Aβ_{5-12} (A) or 0.9 mM Cu(II) and 1.0 mM Aβ_{5-12F} (B) at pH values color coded on the graphs.
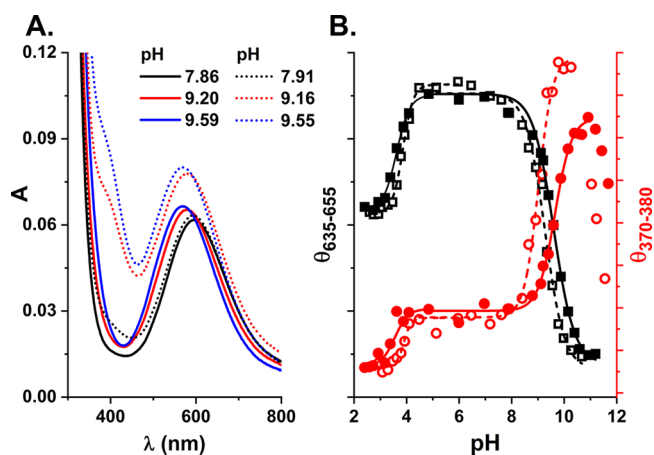

Figure 6. (A) Comparison of UV−vis spectra of Cu(II) complexes of spectra recorded at 25 °C for 0.9 mM Cu(II) and 1.0 mM Aβ_{5-12F} (solid lines) or Aβ_{5-12} (dotted lines) at pH values indicated on the graph. (B) pH dependence of CD signals at 370−380 nm (red circles) or 635−655 nm (black squares) derived from CD spectra shown in Figure 5 for 0.9 mM Cu(II) and 1.0 mM Aβ_{5-12F} (full symbols) or Aβ_{5-12} (open symbols).

we can assign the deprotonation event about pH 9 (8.89(3) from CD, 8.95(7) from UV−vis) to deprotonation and equatorial Cu(II) coordination of Tyr10 phenolate oxygen.[36,37] This band disappears gradually above pH 9.5, in accord with another deprotonation, which can thus be assigned to the replacement of Tyr O$^-$ by the solution-derived OH$^-$ group, with pK_a = 9.92(5). At very high pH an imidazole bridged species is formed as in Cu(II)-Aβ_{5-9}.

The comparison of pK_a values for uncoordinated Tyr, 10.08, coordinated Tyr, 8.89, and deprotonated water in Cu(II)-Aβ_{5-12}, 9.92 vs 9.3 for Cu(II)-Aβ_{5-9} (average of potentiometric and spectroscopy calculations) and 9.62(3) in Aβ_{5-12F} (from spectroscopy), allowed us to estimate the ratio of Cu(II) affinities of Tyr phenolate vs the hydroxyl group at pH 9 as ca. 8.3. The physiological relevance of this interaction is limited, however, as the Cu(II) occupancy by Tyr phenolate at pH 7.4 is 3% or less, estimated from potentiometric data compared to fluorescence titrations of Aβ_{5-12} and Cu(II)-Aβ_{5-12} (Figure S4).

Aβ_{5-16} Complexes. A further C-terminal peptide sequence extension by residues 13−16, VHHQK, added three proton-exchanging side chains, compared to Aβ_{5-12}, His13, His14, and Lys16. As a result, the separation of contributions to potentiometric macroconstants of Tyr10 and Lys16 on one hand and of His6, His13, and His14 on another was not possible, due to overlapping protonation processes. The differences between the respective pK_a values, presented in Table 1, are close to statistical values for two and three equivalent groups, 0.6 and 0.48 pH units, respectively.[31] All these values remain in their typical ranges.

Due to the presence of two distinct Cu(II) binding sites in Aβ_{5-16}, the spectroscopic and potentiometric experiments were performed at the 1.8:1 Cu(II):peptide ratio, in addition to the 0.9:1 ratio used for shorter analogs. The CD titration for the 0.9:1 ratio is presented in Figure 7, the UV−vis titration in Figure S5, and the species distribution plots in Figure 8. The respective data for the 1.8:1 ratio are presented in Figures S6, S7, and S8.
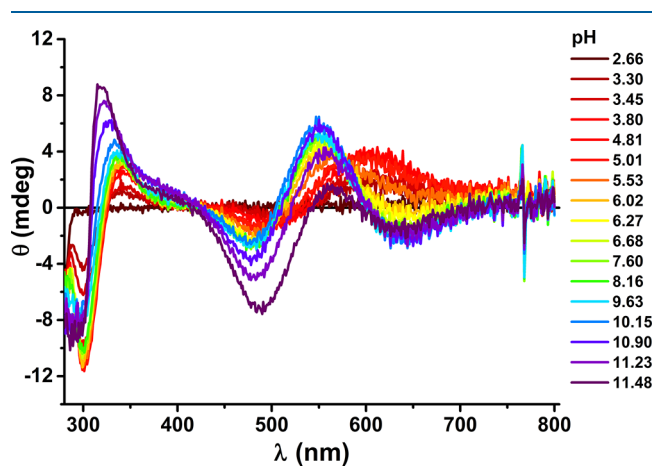

Figure 7. PH dependence of CD spectra recorded at 25 °C for 0.9 mM Cu(II) and 1.0 mM Aβ_{5-16}, at pH values color coded on the graph.
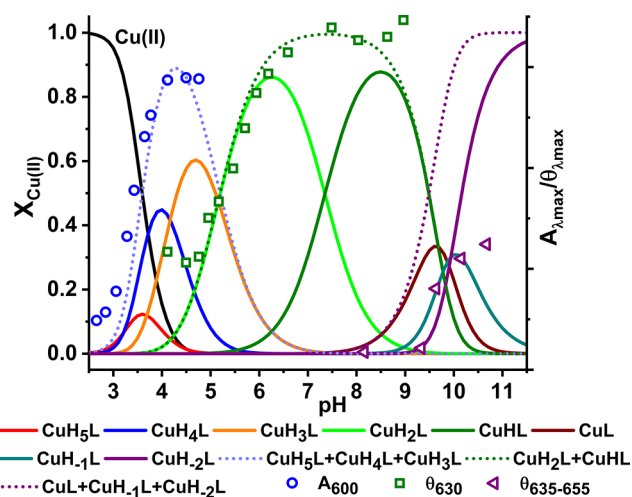

Figure 8. Species distribution calculated for 0.9 mM Cu(II) and 1.0 mM Aβ_{5-16}, on the basis of constants presented in Tables 1 and 2, with selected spectroscopic parameters of Aβ_{5-16} overlaid.
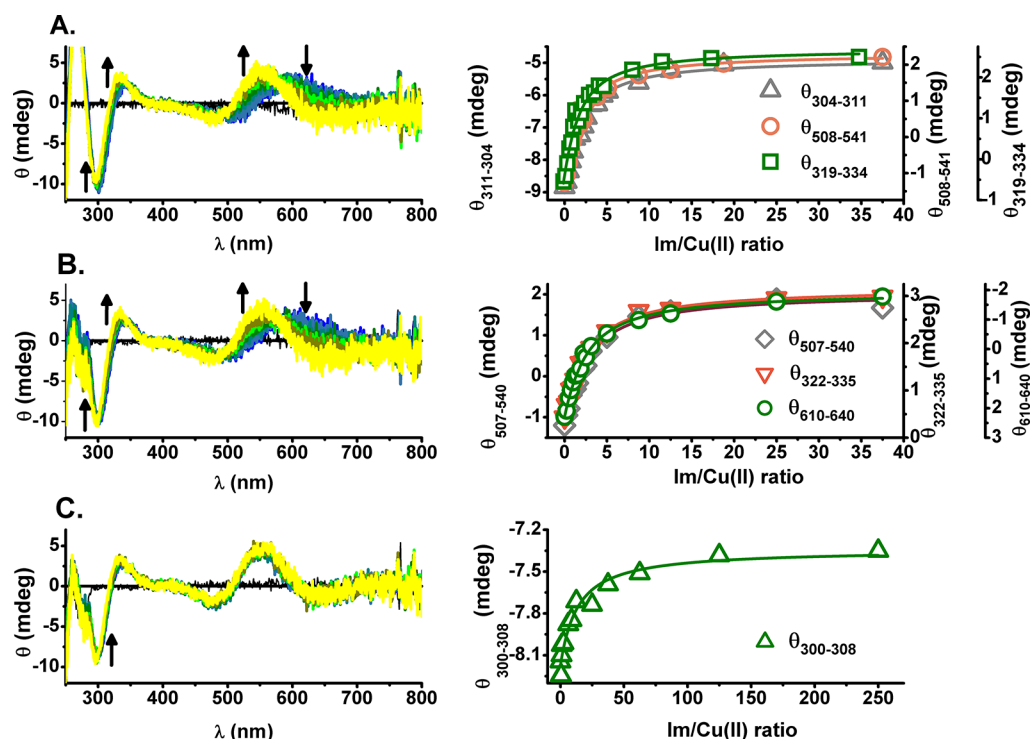
Figure 9. CD titrations and resulting titration curves for Cu(II) complexes of $A\beta_{5-9}$ (A), $A\beta_{5-12}$ (B), and $A\beta_{5-16}$ (C) with imidazole (Im) for 1 mM $A\beta_{5-x}$ and 0.8 mM Cu(II) at pH 7.4. The increasing Im concentrations are color-coded from blue to yellow. The directions of changes are marked by arrows. The titration curves were generated by averaging spectral intensities over the given wavelength ranges for better signal-to-noise ratios. There were no spectral changes in the $d-d$ range for $A\beta_{5-16}$.

At the 0.9:1 ratio the CuH_5L and CuH_4L and CuH_3L complexes present at low pH correspond to the 3N complex. Its spectroscopic parameters with d−d bands at 600 nm at the UV−vis spectrum as well as at 506 and 605 nm at the CD spectrum are very similar to those observed for the 3N complexes of $A\beta_{5-9}$ and $A\beta_{5-12}$. The pK_a of formation of this complex calculated from spectroscopic and potentiometric data is 3.4−3.6. This spectroscopic species is superseded with another, comprising the CuH_2L and $CuHL$ stoichiometries, which exhibited a 35 nm blue shift of the $d-d$ band in the UV−vis spectra and significant changes in the CD pattern (see Table 3, Figure 7, and Figure S5). The pK_a of this process derived from spectroscopy is 5.55. The only residues that can release a proton in this pH range are His13 and His14. These residues are essentially equivalent in the apopeptide, but their pK_a values in the complex are 5.16 and 7.35. These features clearly indicate that His13 or His14 replaces the water molecule in the fourth equatorial coordination site. This observation is further supported by the lack of Tyr phenolate coordination (the absence of a 400 nm band) above pH 8 in Cu(II)-$A\beta_{5-16}$. As a result the Cu(II)-independent Tyr10 and Lys16 deprotonations occur at pH 9.5−10, along with the third proton release, which must originate from the replacement of N^{im} by OH^- in the fourth site. This replacement induces a small change in CD spectra as shown in Figure 8, indicating that the pK_a for this process is ca. 9.65, about 0.3 log units higher than in Cu(II)-$A\beta_{5-9}$. As for all other $A\beta_{5-x}$ peptides a major spectral change above pH 11 was noted, tentatively assigned to the formation of the imidazole bridged tetramer. The protonic equivalence of His13 and His14 and their similar distancing to the N-terminally coordinated Cu(II) ion suggests that the 3 + 1N complex is

actually a mixture of His13 and His14 coordinated species, perhaps with a slight distance-wise preference for His13.

The experiments performed at the Cu(II) excess indicate that the 3N complex is formed in a fashion similar to that at the 1:1 ratio, but it is followed by the additive formation of a novel spectral band (∼579 nm) with the pK_a of 5.90. This complex is analogous to that observed before for Cu(II)-$A\beta_{4-16}$ and corresponds to an independent formation of the second Cu(II) ion at the His13 and His14 residues.[16] As expected, the binding of the second Cu(II) ion at His13/His14 prevented the entry of His13/His14 N^{im} to the coordination sphere of the N-terminal 3N complex.

Ternary Complexes. To further investigate the role of the fourth equatorial site in Cu(II) coordination of $A\beta_{5-x}$ peptides, we performed CD titrations of Cu(II)-$A\beta_{5-9}$/$A\beta_{5-12}$/$A\beta_{5-16}$ complexes with imidazole (Im). The respective CD spectra and titration curves are provided in Figure 9.

The addition of Im resulted in a blue-shift of $d-d$ bands of Cu(II)-$A\beta_{5-9}$/$A\beta_{5-12}$ from 600 to 550 nm as shown in Figure 9A and 9B, respectively. These changes were accompanied by a 10 nm blue-shift and an increase of intensity of CT bands at 340 and 300 nm. No changes in the $d-d$ bands and only a slight effect in CT signals were noticed during the analogous titration of Cu(II)-$A\beta_{5-16}$ (see Figure 9C), even at the final 250-fold excess of Im over Cu(II).

The effects seen for Cu(II)-$A\beta_{5-9}$/$A\beta_{5-12}$ complexes were analogous to those seen previously for Im titrations of all Xaa-His peptides studied by us recently, including WHWSKNR-NH_2, GHTD-NH_2, and GHK[20,21,38] and are consistent with the replacement of the equatorially coordinated water molecule in the 3N coordination mode (N^{am}, N^{im}, N^-) dominant at pH 7.4, with the Im nitrogen, forming the ternary
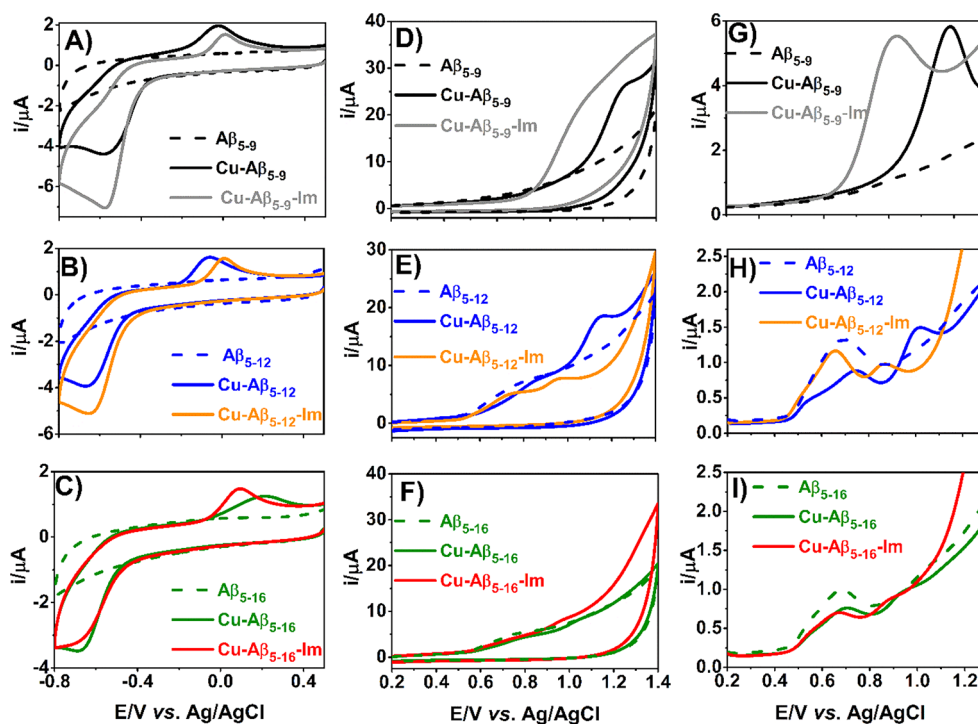
Figure 10. CV (A−F) and DPV (G−I) curves of 0.5 mM Aβ_{5-9} (A, D, G), Aβ_{5-12} (B, E, H), and Aβ_{5-16} (C, F, I) recorded in the absence (dashed line) or the presence of 0.40 mM Cu(II) and 5.0 mM imidazole, pH 7.4.

Table 6. Properties of Redox Processes from CV and DPV Curves of Aβ_{5-x} Binary and Ternary Complexes[a]

Complex	Cu(II)/Cu(I)				Cu(II)/Cu(III)		
	E_{CV}^{RED}	E_{CV}^{OX}	E_{DPV}	I_{DPV} (μA)	E_{CV}^{OX}	E_{DPV}	I_{DPV} (μA)
Cu(II)-Aβ_{5-9}	−0.579(5)	−0.025(1)	−0.453(5)	−1.318(4)	1.297(2)	1.184(4)	2.77(5)
Cu(II)-Aβ_{5-9}-Im	−0.576(1)	0.011(4)	−0.492(1)	−1.490(7)	1.094(5)	1.024(2)	2.918(9)
Cu(II)-Aβ_{5-12F}	−0.633(5)	0.054(3)	−0.540(1)	−1.473(6)	1.269(5)	1.158(2)	3.02(5)
Cu(II)-Aβ_{5-12}	−0.669(1)	−0.062(2)	−0.523(2)	−1.037(5)	1.159(2)	1.018(2)	0.469(5)
Cu(II)-Aβ_{5-12}-Im	−0.647(3)	0.008(3)	−0.516(1)	−1.000(6)	0.955(4)	0.863(2)	0.145(1)
Cu(II)-Aβ_{5-16}	−0.680(4)	0.200(5)	−0.557(2)	−0.434(5)	1.058(4)	0.938(3)	0.065(4)
Cu(II)-Aβ_{5-16}-Im	−0.688(2)	0.093(2)	−0.560(6)	−0.383(7)	0.973(1)	0.876(6)	0.052(2)

[a]E values are given in V vs Ag/AgCl.

3N+1N (N^{am}, N^{imHis6}, N$^-$+ N^{Im}) complex. The same effects were observed for titrations of 3N complexes with the excess of the parent peptide for GHTD-NH$_2$ and GHK[21,38] and Aβ_{5-9} in this work. The much less pronounced response of Cu(II)-Aβ_{5-16} to Im can be readily explained by the intramolecular 3 + 1N coordination in this complex, employing His13/His14 residues. Nevertheless, a slight change of intensity of the CT band at 304 nm, along with the absence of changes in d−d bands can be ascribed to the forced replacement of the intramolecular ligand by external Im. The conditional stability constants (K_T) for Im binding to Cu(II)-Aβ_{5-x} complexes were obtained by global fitting of multiple titration curves according to eq 3:

$$K_T = \frac{[CuL(Im)]}{[CuL][Im]} \tag{3}$$

where L is the Aβ_{5-x} peptide from the initial binary Cu(II) complex.

The K_T values are provided in Table 4. The strongest ternary complex was formed for Cu(II)-Aβ_{5-9} followed by Cu(II)-Aβ_{5-12}. The lower K_T for the latter could be caused by steric

hindrance from additional residues in the Aβ_{5-12} sequence. Such effect is evident in the 3-fold lower K_T for the second Aβ_{5-9} molecule, compared to Im. A further 5-fold lowering of K_T for Cu(II)-Aβ_{5-16} compared to Cu(II)-Aβ_{5-12} is apparently a combination of additional hindrance and the competition from the intramolecular His13/His14 binding. The comparison of ^CK values presented in Table 4 indicates that this interaction increases the overall Cu(II) affinity of Aβ_{5-16} by 1.8 times. This value is in excellent agreement with that derived from the 0.33 pH units shift of OH$^-$ coordination (Aβ_{5-9} vs Aβ_{5-16}, 2.1 times). Therefore, the lowering of Im affinity to Cu(II)-Aβ_{5-16} is a combination of competition between Im and His13/His14 and the increased hampering of Im access to the Cu(II) binding site.

Additionally, we performed a titration of Cu(II)-Aβ_{5-9} with Aβ_{1-16} (SI, Figure S9). Partial precipitation of the ternary complex limited the accuracy of the $^TK_{7.4}$ determination, which was estimated as 5200 M^{-1} (Table 4). This high stability compared to other ternary complexes of Cu(II)-Aβ_{5-x} can be attributed in part to the presence of three His imidazole ligands in Aβ_{1-16} available for the binding, and in part to intermolecular interactions between the Cu(II)-Aβ_{5-9} pep-

tides. We also attempted the study of the Cu(II)-Aβ_{5-16} + Aβ_{1-16} system, but it was precluded by poor solubility of the ternary complex and the apparently weak interaction.

Voltammetry. For further characterization of Aβ_{5-x} peptides, their binary Cu(II) complexes, and ternary complexes with Im, we performed a series of electrochemical experiments using cyclic voltammetry (CV) and differential pulse voltammetry (DPV). The CV results for Aβ_{5-9}, Aβ_{5-12}, and Aβ_{5-16} are presented in Figure 10, with auxiliary CV results for Aβ_{5-12F} provided in Figure S10. All apo-peptides were electrochemically inactive in the studied range of potentials (initially scanning from 0.5 V toward the negative direction, Figure 10A−C, black, blue, green, dashed lines; gray dashed line in Figure S10A), except for broad peaks observed at 0.6−0.9 V for Aβ_{5-12} and Aβ_{5-16} (Figure 10E−F, H−I, blue and green dashed lines) assigned to the Tyr10 phenol ring oxidation to a thermodynamically unstable tyrosyl radical subsequently converted into orthoquinone.[40−42] Aβ_{5-9} and Aβ_{5-12F} were redox silent in this range, as expected (Figure 10D, G; Figure S10B).

The 3N Cu(II)-Aβ_{5-x} complexes yielded irreversible reduction peaks in voltammograms recorded from +0.5 V to −0.8 V (Figure 10A−C, Figure S11, black, blue, and green solid lines and Figure S10A, gray solid line, see Table 6 for CV and DPV-derived potentials). A significant separation between the cathodic and anodic peaks suggests a slow electron transfer and/or a reorganization of the complex structure upon Cu(II) reduction. This can be explained by the incompatibility of the planar 3N chelate of Aβ_{5-x} peptides with geometrical preferences of Cu(I) ions, as pointed out previously by Hureau et al. in their Cu(II)-GHK study.[19] The cathodic peak of Cu(II)-Aβ_{5-16} had an altered shape, appeared at the most negative potential, and had the lowest peak current (Figure 10C green solid line, Table 6). These effects are compatible with the formation of the 3 + 1N coordination structure supplanted by the His-13/His-14 imidazole nitrogen.

The Cu(II)-Aβ_{5-x} complexes can generate a Cu(II)/Cu(III) redox couple at potentials around 1 V and higher (Figure 10D−I (black, blue, and green solid lines) and Figure S10B (solid gray line)). For binary Cu(II)-Aβ_{5-x} complexes with Tyr-containing peptides, the Cu(II)/Cu(III) redox signal was preceded by Tyr10 oxidation peaks of decreased intensity and shifted to more positive potentials relative to apopeptides, in agreement with the literature.[41] The lack of Cu(III)/Cu(II) reduction peaks in the studied complexes may be attributed to the catalytic oxidation of peptide ligands *via* the electrogenerated (highly oxidizing) Cu(III) species according to an EC (electrochemical-chemical) mechanism. In addition to the Tyr phenolic ring, His imidazoles in Cu(II)-Aβ_{5-16} can also be oxidized by Cu(III) at such potentials, (E^{ox} ∼ 1.25 V for L-His[42] and ∼1.0 V for His in Aβ42/Aβ16[43]). The use of faster scan rates (0.5−5 V/s) did not improve the reversibility of the studied process (data not shown). The EC mechanism explains the irreversibility of these Cu(II)/Cu(III) couples, in contrast to the reversible Cu(II)/Cu(III) process in Aβ_{4-8} and Aβ_{4-10F} complexes.[44] The potentials of Cu(II)/Cu(III) peaks for Aβ_{5-x} complexes appeared in the following decreasing order: Cu(II)-Aβ_{5-16} > Cu(II)-Aβ_{5-12} > Cu(II)-Aβ_{5-12F} > Cu(II)-Aβ_{5-9} (see Table 6 for values). Additionally, the intensity of the oxidation current increased in the same sequence.

Finally, electrochemical measurements for ternary Im complexes of Cu(II)-Aβ_{5-x} were done (Figure 10A−I, gray, orange, and red solid lines). A 12.5-fold Im excess over Cu(II)

excess was used to ensure full saturation of Cu(II) with Im for Cu(II)-Aβ_{5-9} and Cu(II)-Aβ_{5-12} and 50% saturation for Aβ_{5-16}, according to equilibrium titrations. No significant changes in the voltammetric signature were noticed in the range of negative potentials (Figure 10A−C, Figure S11), but according to CV and DPV curves registered in the 0.2−1.3 V potential range (Figure 10D−I), the Im addition shifted both the Cu(II)/Cu(III) and Tyr10 oxidation toward less positive potentials. This is in accord with the presence of the 3 + 1N coordination of Cu(II) in the ternary complex, which stabilizes Cu(III) better.[45] The largest shifts in electrochemical responses occurred for Cu(II)-Aβ_{5-9}-Im and Cu(II)-Aβ_{5-12}-Im in relation to the binary complexes. In contrast, a weaker interaction between Cu(II)-Aβ_{5-16} and imidazole due to the presence of the autoternary complex resulted in a smaller change in redox activity of this chelate. Still, the potentials of formation of Cu(III) species are probably too high to have a biological relevance.

Cu(II) Exchange and Biological Relevance. The stability of a complex is a key property in considering its biological relevance, as biological fluids are teeming with small molecules and proteins ready to compete for copper. Aβ peptides are essentially extracellular, and their toxicity is exerted mostly in synapses. Not much is known quantitatively about the fast-changing composition of synaptic cleft fluid. Therefore, we are forced to make educated guesses regarding Cu(II) complexation by Aβ peptides. The Aβ_{1-x} family peptides bind the Cu(II) ion with log $^{C}K_{7.4}$ = 10.04 (x = 16) and 10.43 (x = 40).[46] Much higher Cu(II) affinities were determined for Aβ_{4-x} family peptides,[8] log $^{C}K_{7.4}$ = 13.53 (x = 16),[16] and 14.18 (x = 9).[47] The affinities of binary Cu(II)-Aβ_{5-x} peptides are closer to Cu(II)-Aβ_{4-x}, log $^{C}K_{7.4}$ = 12.76 (x = 9), and 12.98 (x = 16). However, unlike Aβ_{4-x}, the Aβ_{5-x} peptides can elevate their Cu(II) binding capability via ternary complexes, which is a feature shared with other Xaa-His peptides.[17,20,21,37] Figure 11 presents the evolution of log $^{C}K_{7.4}$ of ternary Im and Aβ_{1-16} complexes of Cu(II)-Aβ_{5-9} and Cu(II)-Aβ_{5-16} calculated using the data presented in Tables 1, 2, and 4.

This simulation clearly shows that in the presence of a ∼1 mM amount of external imidazole-bearing ligands Aβ_{5-9} can become a stronger Cu(II) chelator than the longer Aβ_{5-x} species. Furthermore, at ca. 30 mM Im the Cu(II) binding ability of Aβ_{5-16} equals that of Aβ_{4-16}, and that of Aβ_{5-9}
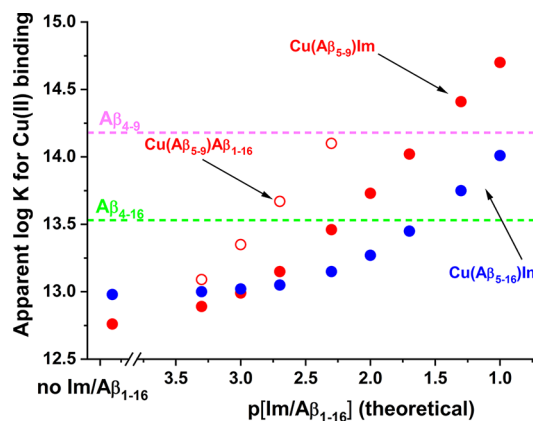

Figure 11. Theoretical evolution of log $^{C}K_{7.4}$ of ternary complexes Cu(II)-Aβ_{5-9}/Im, Cu(II)-Aβ_{5-16}/Im, and Cu(II)-Aβ_{5-9}/Aβ_{1-16} calculated using the data presented in Tables 1, 2, and 4.

matches $A\beta_{4-9}$. While the actual role of $A\beta_{4-x}$ peptides in brain copper metabolism remains speculative, we postulate that the longer species serve to mop up the excess of Cu(II) ions from the synaptic cleft,[18] and $A\beta_{4-9}$, as product of $A\beta_{4-40}$ cleavage by neprilysin may participate in the export of copper across the blood−brain barrier.[48,49] $A\beta_{5-x}$ peptides are normally only very minor contributors to the overall β-amyloid pool but our results indicate that these peptides, when multiplicated as a result of therapeutic intervention, may interfere with the synaptic and extrasynaptic Cu(II) handling. The affinity of the Cu(II)-$A\beta_{5-9}$/$A\beta_{1-16}$ complex, much higher than that of imidazole, points at a possibility of strong, specific interactions with larger ligands that can be recruited from the $A\beta$ family or other synaptic proteins. Despite the similar overall affinity, Cu(II)-Xaa-His and Cu(II)-Xaa-Zaa-His (ATCUN) complexes differ in the Cu(II) exchange kinetics, with Cu(II)-Xaa-His complexes reported as much more labile.[50] They could thus interfere with proper Cu(II) delivery. In particular, $A\beta_{5-9}$ which most likely could be generated by neprilysin analogously to $A\beta_{4-9}$, could theoretically intercept Cu(II) ions faster than the ATCUN peptides and release them off target, e.g. intracellularly, causing oxidative stress in brain cells.[49]

In order to directly find out how $A\beta_{5-x}$ and $A\beta_{4-x}$ peptides could compete for Cu(II) ions, we contacted them directly, by forming the Cu(II)-$A\beta_{5-9}$ complex at pH 7.4 and then contacting it with equimolar $A\beta_{4-9}$. The reaction was then followed for 24 h, as presented in Figure 12.
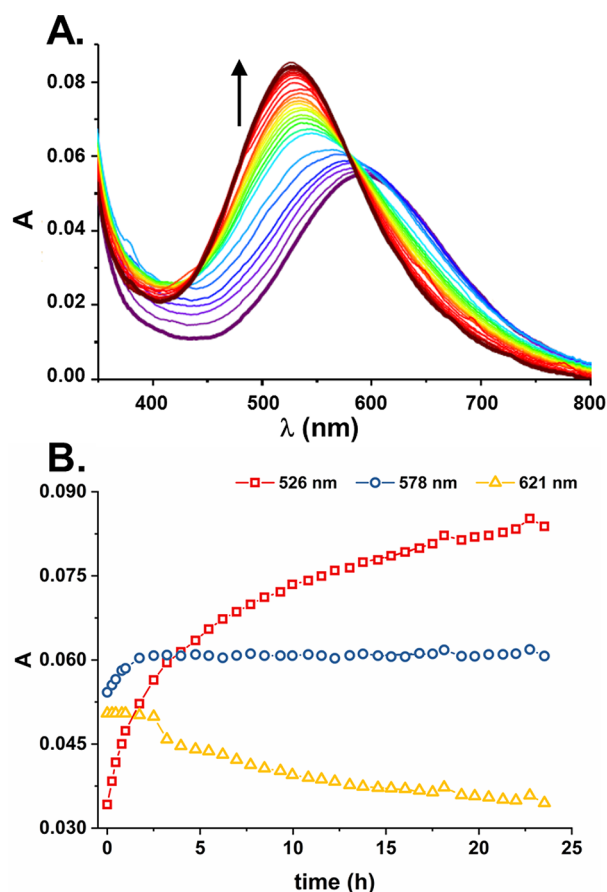

Figure 12. Course of reaction of 1 mM Cu(II)-$A\beta_{5-9}$ with 1 mM $A\beta_{4-9}$ at pH 7.4 (20 mM HEPES) at 25 °C: (A) evolution of $d-d$ bands; (B) reaction traces at 526, 578, and 621 nm.

By comparing its course with the spectra presented above and with those published previously by Bossak-Ahmad et al.[47] one can clearly see that the process of Cu(II) transfer from $A\beta_{5-x}$ to $A\beta_{4-x}$, along the gradient of affinities, is mediated by the formation of the ternary 3N+$N_{A\beta(4-9)}$ complex. Interestingly, however, the overall process, measured at the maximum of Cu(II)-$A\beta_{4-x}$ absorption, was very slow, taking more than 24 h to complete. Even more interestingly, the reaction had not one, but two slow steps. The first one, taking the first 2.5 h of incubation and characterized by an isosbestic point at 621 nm, was apparently the formation of the ternary complex, which then re-equilibrated into the final 4N Cu(II)-$A\beta_{4-9}$ species with the isosbestic point at 578 nm. This experiment shows that the formation of ternary complexes can stabilize the Cu(II)-$A\beta_{5-x}$ complexes not just thermodynamically, but also kinetically. Taking into account the milliseconds to seconds to minutes time scale of chemical processes in the synapses, such slow equilibrations between $A\beta_{5-x}$ and $A\beta_{4-x}$ indicate that ternary Cu(II)-$A\beta_{5-x}$ complexes with external ligands, including other $A\beta$ peptides, may indeed interfere with copper brain physiology.

Electrochemical properties of Cu(II)-$A\beta_{5-x}$ complexes may further contribute to the impairment of brain copper metabolism by enabling the Cu(II)/Cu(I) cycle in the high-affinity Cu(II) pool, not accessible to much weaker Cu(II)-$A\beta_{1-x}$ complexes. In this fashion the overproduction of $A\beta_{5-x}$ peptides could also enhance the oxidative stress and reactive oxygen species (ROS) generation, normally ascribed to Cu(II)-$A\beta_{1-x}$ species.[51−53] On the other hand, the oxidation of Cu(II) ions in $A\beta_{5-x}$ complexes to Cu(III) is even less likely than in $A\beta_{4-x}$ complexes, but the presence of imidazole shifted the oxidation potential of the Cu(II)/Cu(III) couple toward less positive potential values, thus slightly increasing the probability of this reaction *in vivo*. Taken together, our results indicate that $A\beta_{5-x}$ peptides, which bind Cu(II) ions much more strongly than $A\beta_{1-x}$ peptides[46] and only slightly more weakly than $A\beta_{4-x}$ peptides,[16,47] could interfere with Cu(II) handling by these peptides, adding to copper dyshomeostasis in Alzheimer brains, especially in the presence of auxiliary imidazole ligands, such as His side chains in other peptides and proteins.

■ ASSOCIATED CONTENT

ⓈI Supporting Information

The Supporting Information is available free of charge at https://pubs.acs.org/doi/10.1021/acs.inorgchem.0c01773.

> pH dependence of UV−vis spectra for Cu(II)-$A\beta_{5-x}$ samples, fluorescence titrations of $A\beta_{5-12}$ and Cu(II)-$A\beta_{5-12}$, spectroscopic results and species distribution for 1 mM $A\beta_{5-16}$ and 1.8 mM Cu(II), spectroscopic titration of Cu(II)-$A\beta_{5-9}$ with $A\beta_{1-16}$, CV for $A\beta_{5-12F}$/Cu(II)-$A\beta_{5-12F}$, and DPV for $A\beta_{5-x}$/Cu(II)/Im over 0.2 to −0.8 V potential range (PDF)

■ AUTHOR INFORMATION

Corresponding Author

Wojciech Bal − *Institute of Biochemistry and Biophysics, Polish Academy of Sciences, 02-106 Warsaw, Poland;* ◉ orcid.org/0000-0003-3780-083X; Email: wbal@ibb.waw.pl

Authors

Nina E. Wezynfeld − *Chair of Medical Biotechnology, Faculty of Chemistry, Warsaw University of Technology, 00-664 Warsaw, Poland;* ◉ orcid.org/0000-0002-6206-4195

Aleksandra Tobolska − *Chair of Medical Biotechnology, Faculty of Chemistry, Warsaw University of Technology, 00-664 Warsaw, Poland; Faculty of Chemistry, University of Warsaw, 02-093 Warsaw, Poland;* ◉ orcid.org/0000-0002-4643-7000

Mariusz Mital − *Institute of Biochemistry and Biophysics, Polish Academy of Sciences, 02-106 Warsaw, Poland*

Urszula E. Wawrzyniak − *Chair of Medical Biotechnology, Faculty of Chemistry, Warsaw University of Technology, 00-664 Warsaw, Poland*

Magdalena Z. Wiloch − *Charge Transfer Processes in Hydrodynamic Systems Group, Institute of Physical Chemistry, Polish Academy of Sciences, 01-224 Warsaw, Poland*

Dawid Płonka − *Institute of Biochemistry and Biophysics, Polish Academy of Sciences, 02-106 Warsaw, Poland;* ◉ orcid.org/0000-0002-4076-9231

Karolina Bossak-Ahmad − *Institute of Biochemistry and Biophysics, Polish Academy of Sciences, 02-106 Warsaw, Poland*

Wojciech Wróblewski − *Chair of Medical Biotechnology, Faculty of Chemistry, Warsaw University of Technology, 00-664 Warsaw, Poland*

Complete contact information is available at:
https://pubs.acs.org/10.1021/acs.inorgchem.0c01773

Notes

The authors declare no competing financial interest.

■ REFERENCES

(1) Alzheimer's Disease International. *World Alzheimer Report* 2019. Attitudes to dementia. www.alz.co.uk/research/WorldAlzheimerReport2019.pdf.

(2) Haaksma, M. L.; Vilela, L. R.; Marengoni, A.; Calderón-Larrañaga, A.; Leoutsakos, J.-M. S.; Olde Rikkert, M. G. M.; Melis, R. J. F. Comorbidity and Progression of Late Onset Alzheimer's Disease: A Systematic Review. *PLoS One* 2017, 12 (5), No. e0177044.

(3) He, Y.; Wei, M.; Wu, Y.; Qin, H.; Li, W.; Ma, X.; Cheng, J.; Ren, J.; Shen, Y.; Chen, Z.; Sun, B.; Huang, F. D.; Shen, Y.; Zhou, Y. D. Amyloid β oligomers suppress excitatory transmitter release via presynaptic depletion of phosphatidylinositol-4,5-bisphosphate. *Nat. Commun.* 2019, 10, 1193.

(4) Zott, B.; Simon, M. M.; Hong, W.; Unger, F.; Chen-Engerer, H.-J.; Frosch, M. P.; Sakmann, B.; Walsh, D. M.; Konnerth, A. A vicious cycle of amyloid β-dependent neuronal hyperactivation. *Science* 2019, 365, 559−565.

(5) Mattsson, N.; Rajendran, L.; Zetterberg, H.; Gustavsson, M.; Andreasson, U.; Olsson, M.; Brinkmalm, G.; Lundkvist, J.; Jacobson, L. H.; Perrot, L.; Neumann, U.; Borghys, H.; Mercken, M.; Dhuyvetter, D.; Jeppsson, F.; Blennow, K.; Portelius, E. BACE1 inhibition induces a specific cerebrospinal fluid β-amyloid pattern that identifies drug effects in the central nervous system. *PLoS One* 2012, 7 (2), No. e31084.

(6) Lewis, H.; Beher, D.; Cookson, N.; Oakley, A.; Piggott, M.; Morris, C. M.; Jaros, E.; Perry, R.; Ince, P.; Kenny, R. A.; Ballard, C. G.; Shearman, M. S.; Kalaria, R. N. Quantification of Alzheimer pathology in ageing and dementia: Age-related accumulation of amyloid-beta(42) peptide in vascular dementia. *Neuropathol. Appl. Neurobiol.* 2006, 32, 103−118.

(7) Murayama, K. S.; Kametani, F.; Tabira, T.; Araki, W. A novel monoclonal antibody specific for the amino-truncated beta-amyloid Abeta5−40/42 produced from caspase-cleaved amyloid precursor protein. *J. Neurosci. Methods* 2007, 161, 244−249.

(8) Portelius, E.; Bogdanovic, N.; Gustavsson, M. K.; Volkmann, I.; Brinkmalm, G.; Zetterberg, H.; Winblad, B.; Blennow, K. Mass spectrometric characterization of brain amyloid beta isoform signatures in familial and sporadic Alzheimer's disease. *Acta Neuropathol.* 2010, 120, 185−193.

(9) Wirths, O.; Zampar, S.; Weggen, S. In *N-Terminally Truncated Aβ Peptide Variants in Alzheimer's Disease in Alzheimer's Disease*; Wisniewski, T., Ed.; Codon Publications: Brisbane, Australia, 2019; pp 107−122, ISBN: 978-0-6468096-8-7, DOI: 10.15586/alzheimers-disease.

(10) Gkanatsiou, E.; Portelius, E.; Toomey, C. E.; Blennow, K.; Zetterberg, H.; Lashley, T.; Brinkmalm, G. A distinct brain beta amyloid signature in cerebral amyloid angiopathy compared to Alzheimer's disease. *Neurosci. Lett.* 2019, 701, 125−131.

(11) Reinert, J.; Richard, B. C.; Klafki, H. W.; Friedrich, B.; Bayer, T. A.; Wiltfang, J.; Kovacs, G. G.; Ingelsson, M.; Lannfelt, L.; Paetau, A.; Bergquist, J.; Wirths, O. Deposition of C-terminally truncated Aβ species Aβ37 and Aβ39 in Alzheimer's disease and transgenic mouse models. *Acta Neuropathol. Comm.* 2016, 4, 24.

(12) Portelius, E.; Olsson, M.; Brinkmalm, G.; Ruetschi, U.; Mattsson, N.; Andreasson, U.; Gobom, J.; Brinkmalm, A.; Holtta, M.; Blennow, K. Mass spectrometric characterization of amyloid-β species in the 7PA2 cell model of Alzheimer's disease. *J. Alzheimer's Dis.* 2012, 33, 85−93.

(13) Takeda, K.; Araki, W.; Akiyama, H.; Tabira, T. Amino-truncated amyloid beta-peptide (Abeta5−40/42) produced from caspase-cleaved amyloid precursor protein is deposited in Alzheimer's disease brain. *FASEB J.* 2004, 18 (14), 1755−7.

(14) Drew, S. C.; Barnham, K. J. The Heterogeneous Nature of Cu²⁺ interactions with Alzheimer's Amyloid-β Peptide. *Acc. Chem. Res.* 2011, 44 (11), 1146−1155.

(15) Atrián-Blasco, E.; Gonzalez, P.; Santoro, A.; Alies, B.; Faller, P.; Hureau, C. Cu and Zn Coordination to Amyloid Peptides: From Fascinating Chemistry to Debated Pathological Relevance. *Coord. Chem. Rev.* 2018, 371, 38−55.

(16) Mital, M.; Wezynfeld, N. E.; Frączyk, T.; Wiloch, M. Z.; Wawrzyniak, U. E.; Bonna, A.; Tumpach, C.; Barnham, K. J.; Haigh, C. L.; Bal, W.; Drew, S. C. A Functional Role for Aβ in Metal Homeostasis? N-Truncation and High-Affinity Copper Binding. *Angew. Chem., Int. Ed.* 2015, 54, 10460−10464.

(17) Gonzalez, P.; Bossak, K.; Stefaniak, E.; Hureau, C.; Raibaut, L.; Bal, W.; Faller, P. N-terminal Cu Binding Motifs Xxx-Zzz-His (ATCUN) and Xxx-His and their derivatives: Chemistry, Biology and Medicinal Applications. *Chem. - Eur. J.* 2018, 24, 8029−8041.

(18) Stefaniak, E.; Bal, W. Cu^II binding properties of N-truncated Aβ peptides: in search of biological function. *Inorg. Chem.* 2019, 58, 13561−13577.

(19) Hureau, C.; Eury, H.; Guillot, R.; Bijani, C.; Sayen, S.; Solari, P. L.; Guillon, E.; Faller, P.; Dorlet, P. X-ray and solution structures of Cu(II) GHK and Cu(II) DAHK complexes: influence on their redox properties. *Chem. - Eur. J.* 2011, 17, 10151−10160.

(20) Bossak, K.; Mital, M.; Poznański, J.; Bonna, A.; Drew, S.; Bal, W. Interactions of α-factor-1, a yeast pheromone, and its analog with copper(II) ions and low molecular weight ligands yield very stable complexes. *Inorg. Chem.* 2016, 55, 7829−7831.

(21) Kotuniak, R.; Frączyk, T.; Skrobecki, P.; Płonka, D.; Bal, W. GHTD-amide, an insulin activating peptide from human pancreas is a strong Cu(II) chelator. *Inorg. Chem.* **2018**, *57*, 15507−15516.

(22) Trapaidze, A.; Hureau, C.; Bal, W.; Winterhalter, M.; Faller, P. Thermodynamic study of Cu^{2+} binding to the DAHK and GHK peptides by Isothermal Titration Calorimetry (ITC). *JBIC, J. Biol. Inorg. Chem.* **2012**, *17*, 37−47.

(23) Conato, C.; Gavioli, R.; Guerrini, R.; Kolzowski, H.; Mlynarz, P.; Pasti, C.; Pulidori, F.; Remelli, M. Copper complexes of glycylhistidyl-lysine and two of its synthetic analogues: chemical behavior and biological activity. *Biochim. Biophys. Acta, Gen. Subj.* **2001**, *1526*, 199−210.

(24) Chan, W. C.; White, P. D. In *Fmoc Solid Phase Peptide Synthesis, A Practical Approach*; Chan, W. C., White, P. D., Eds.; Oxford University Press: New York, 2000; pp 41−76.

(25) Kuipers, B. J. H.; Gruppen, H. Prediction of Molar Extinction Coefficients of Proteins and Peptides Using UV Absorption of the Constituent Amino Acids at 214 nm To Enable Quantitative Reverse Phase High-Performance Liquid Chromatography-Mass Spectrometry Analysis. *J. Agric. Food Chem.* **2007**, *55*, 5445−5451.

(26) Irving, H. M.; Miles, M. G.; Pettit, L. D. A study of some problems in determining the stoicheiometric proton dissociation constants of complexes by potentiometric titrations using a glass electrode. *Anal. Chim. Acta* **1967**, *38*, 475−488.

(27) Gans, P.; Sabatini, A.; Vacca, A. SUPERQUAD: an improved general program for computation of formation constants from potentiometric data. *J. Chem. Soc., Dalton Trans.* **1985**, 1195−1199.

(28) Gans, P.; Sabatini, A.; Vacca, A. Investigation of equilibria in solution. Determination of equilibrium constants with the HYPER-QUAD suite of programs. *Talanta* **1996**, *43*, 1739−1753.

(29) Kowalik-Jankowska, T.; Ruta, M.; Wiśniewska, K.; Lankiewicz, L. Coordination Abilities of the 1−16 and 1−28 Fragments of Beta-Amyloid Peptide towards Copper(II) Ions: A Combined Potentiometric and Spectroscopic Study. *J. Inorg. Biochem.* **2003**, *95* (4), 270−282.

(30) Damante, C. A.; Ösz, K.; Nagy, Z.; Pappalardo, G.; Grasso, G.; Impellizzeri, G.; Rizzarelli, E.; Sóvágó, I. The Metal Loading Ability of β-Amyloid N-Terminus: A Combined Potentiometric and Spectroscopic Study of Copper(II) Complexes with β-Amyloid(1−16), Its Short or Mutated Peptide Fragments, and Its Polyethylene Glycol (PEG)-ylated Analogue. *Inorg. Chem.* **2008**, *47*, 9669−9683.

(31) Szakács, Z.; Kraszni, M.; Noszál, B. Determination of microscopic acid−base parameters from NMR−pH titrations. *Anal. Bioanal. Chem.* **2004**, *378*, 1428−1448.

(32) Daniele, P.; Zerbinati, O.; Zelano, V.; Ostacoli, G. Thermodynamic and spectroscopic study of copper(II)-glycyl-L-histidylglycine complexes in aqueous solution. *J. Chem. Soc., Dalton Trans.* **1991**, 2711−2715.

(33) Farkas, E.; Sóvágó, I.; Kiss, T.; Gergely, A. Studies on transition-metal-peptide complexes. Part 9. Copper(II) complexes of tripeptides containing histidine. *J. Chem. Soc., Dalton Trans.* **1984**, 611−614.

(34) Brookes, G.; Pettit, L. Thermodynamics of formation of complexes of copper(II) and nickel(II) ions with glycylhistidine, β-alanylhistidine, and histidylglycine. *J. Chem. Soc., Dalton Trans.* **1975**, 2106−2112.

(35) Arena, G.; Cucinotta, V.; Musumeci, S.; Purrello, R.; Rizzarelli, E. Formation and stability of simple and mixed complexes of glycyl-L-histidine in aqueous solution. *Ann. Chim. (Rome)* **1984**, *74*, 399−402.

(36) Pettit, L. D.; Steel, I.; Kowalik, T.; Kozlowski, H.; Bataille, M. Specific binding of the tyrosine residue in copper(II) complexes of Tyr-Pro-Gly-Tyr and Tyr-Gly-Pro-Tyr. *J. Chem. Soc., Dalton Trans.* **1985**, 1201−1205.

(37) Livera, C.; Pettit, L. D.; Bataille, M.; Krembel, J.; Bal, W.; Kozlowski, H. Copper(II) complexes with some tetrapeptides containing the 'break-point' prolyl residue in the third position. *J. Chem. Soc., Dalton Trans.* **1988**, 1357−1360.

(38) Bossak-Ahmad, K.; Wiśniewska, M. D.; Bal, W.; Drew, S. C.; Frączyk, T. Ternary Cu(II) complex with GHK peptide and cis-

(39) Krężel, A.; Wójcik, J.; Maciejczyk, M.; Bal, W. May GSH and l-His contribute to intracellular binding of zinc? Thermodynamic and solution structural study of a ternary complex. *Chem. Commun.* **2003**, 704−705.

(40) Enache, T. A.; Oliveira-Brett, A. M. Phenol and para-substituted phenols electrochemical oxidation pathways. *J. Electroanal. Chem.* **2011**, *655*, 9−16.

(41) Suprun, E. V.; Zaryanov, N. V.; Radko, S. P.; Kulikova, A. A.; Kozin, S. A.; Makarov, A. A.; Archakov, A. I.; Shumyantseva, V. V. Tyrosine Based Electrochemical Analysis of Amyloid-β Fragment (1−16) Binding to Metal(II) Ions. *Electrochim. Acta* **2015**, *179*, 93−99.

(42) Enache, T. A.; Oliveira-Brett, A. M. Peptide methionine sulfoxide reductase A (MsrA): direct electrochemical oxidation on carbon electrodes. *Bioelectrochemistry* **2013**, *89*, 11−18.

(43) Suprun, E. V.; Khmeleva, S. A.; Radko, S. P.; Kozin, S. A.; Archakov, A. I.; Shumyantseva, V. V. Direct electrochemical oxidation of amyloid-β peptides via tyrosine, histidine, and methionine residues. *Electrochem. Commun.* **2016**, *65*, 53−56.

(44) Wiloch, M. Z.; Wawrzyniak, U. E.; Ufnalska, I.; Bonna, A.; Bal, W.; Drew, S. C.; Wroblewski, W. Tuning the Redox Properties of Copper(II) Complexes with Amyloid-Beta Peptides. *J. Electrochem. Soc.* **2016**, *163* (13), G196−G199.

(45) Ufnalska, I.; Warzyniak, U. E.; Bossak-Ahmad, K.; Bal, W.; Wróblewski, W. Electrochemical studies of binary and ternary copper(II) complexes with α-factor analogues. *J. Electroanal. Chem.* **2020**, *862*, 114003.

(46) Alies, B.; Renaglia, E.; Rózga, M.; Bal, W.; Faller, P.; Hureau, C. Cu(II) affinity for the Alzheimer's peptide: Tyrosine fluorescence studies revisited. *Anal. Chem.* **2013**, *85*, 1501−1508.

(47) Bossak-Ahmad, K.; Mital, M.; Płonka, D.; Drew, S. C.; Bal, W. Oligopeptides Generated by Neprilysin Degradation of β-Amyloid Have the Highest Cu(II) Affinity in the Whole Aβ Family. *Inorg. Chem.* **2019**, *58* (1), 932−943.

(48) Mital, M.; Bal, W.; Frączyk, T.; Drew, S. C. Interplay between copper, neprilysin and N-truncation of β-amyloid. *Inorg. Chem.* **2018**, *57*, 6193−6197.

(49) Stefaniak, E.; Płonka, D.; Szczerba, P.; Wezynfeld, N. E.; Bal, W. Copper transporters? Glutathione reactivity of products of Cu-Aβ digestion by neprilysin. *Inorg. Chem.* **2020**, *59*, 4186−4190.

(50) Beuning, C. K.; Mestre-Voegtlé, B.; Faller, P.; Hureau, C.; Crans, D. C. Measurement of Interpeptidic Cu(II) Exchange Rate Constants by Static Fluorescence Quenching of Tryptophan. *Inorg. Chem.* **2018**, *57*, 4791−4794.

(51) Cheignon, C.; Jones, M.; Atrian-Blasco, E.; Kieffer, I.; Faller, P.; Collin, F.; Hureau, C. Identification of key structural features of the elusive Cu-Ab complex that generates ROS in Alzheimer's disease. *Chem. Sci.* **2017**, *8*, 5107−5118.

(52) Atrian-Blasco, E.; Del Barrio, M.; Faller, P.; Hureau, C. Ascorbate Oxidation by Cu(Amyloid-β) Complexes: Determination of the Intrinsic Rate as a Function of Alterations in the Peptide Sequence Revealing Key Residues for Reactive Oxygen Species Production. *Anal. Chem.* **2018**, *90* (9), 5909−5915.

(53) Cheignon, C.; Tomas, M.; Bonnefont-Rousselot, D.; Faller, P.; Hureau, C.; Collin, F. Oxidative Stress and the Amyloid Beta Peptide in Alzheimer's Disease. *Redox Biol.* **2018**, *14*, 450−464.